Materials Science Forum
ISSN: 1662-9752, Vol. 869, pp 35-39
doi:10.4028/www.scientific.net/MSF.869.35

Submitted: 2016-01-18
Accepted: 2016-03-10
Online: 2016-08-31

Synthesis, Characterization and Photoluminescent Properties of ZrO_2 Nanocrystals

Giancarlo da Silva Sousa[1,a], Laécio Santos Cavalcante[2,b], Maria Rita de M. Santos[3,a,c], José Milton Elias de Matos[4,a]

[1]Federal University of Piaui – UFPI/CCN – Department of Chemistry – interdisciplinary laboratory for advanced materials – LIMAv – Campus University Minister Petrônio Portela, Ininga, Teresina – PI, 64049-550, Brazil, phone (550XX86) 3221 5710.

[2]State University of Piaui – UESPI/CCN – Department of Chemistry – Campus University Torquato Neto, Pirajá, Teresina – PI, 64000-000, Brazil, phone (550XX86) 3221 5710.

[3]Federal University of Piaui – UFPI/CCN – Department of Materials Science - interdisciplinary laboratory for advanced materials – LIMAv – Campus University Minister Petrônio Portela, Ininga, Teresina – PI, 64049-550, Brazil, phone (550XX86) 3221 5710.

[a]gicarlo.gain@gmail.com, [b]laeciosc@bol.com.br, [c]mrita@ufpi.edu.br, [d]jmematos@ufpi.edu.br

Keywords: Zirconium Oxide, Nanoparticles, Morphology, Photoluminescence.

Abstract. Nanocrystalline zirconium oxide (ZrO_2) was synhesized by hydrothermal method in presence of hydrogen peroxide. Surface morphology analysis depicts the formation of the nanorods. The structural analysis confirms that the as-synthesized ZrO2 product is of pure monoclinic phase (m-ZrO_2) with crystallite size of about ~8 nm. The product consists of monodispersed nanoparticles of uniform composition, high purity, and crystallinity. The Raman spectra are quantitatively analyzed and the observed peaks are attributed to various vibration modes of the m-ZrO_2. Photoluminescence (PL) spectrum of ZrO2 nanostructure showed a strong and broad emission peak at around 534 nm, which can be attributed the participation of several energy levels..

Introduction

In recent years, there has been considerable interest in photoluminescent properties of many metal oxides such as TiO_2, ZnO, and and ZrO_2 [1-3]. Among these oxides the zirconium oxide (ZrO_2) is a very interesting material and of fundamental study and application-oriented research. ZrO_2 is a wide band gap (5.0-5.5 eV) transition metal oxide with useful mechanical, thermal, optical, and electrical properties. It has a variety of applications, including solid-state electrolytes, thermal barrier coatings, electro optical materials, and oxygen sensors [4-5]. ZrO_2 exhibits three crystallographic phases with increasing temperature at a normal atmospheric pressure: the monoclinic phase, from room temperature to 1175 °C; the tetragonal phase, from 1175 to 2370 °C; and the cubic phase, from 2370 to 2750 °C (melting point) [6].

The optical properties and especially the photoluminescence (PL) properties of ZrO_2 have been seldom reported, although PL has already been observed in a ZrO_2 sol and nanoparticle systems. [7-8]. There has been an increasing interest in the application of ZrO_2 nanoparticles for photonics systems due to their enhanced luminescent properties associated with their small size [9]. Luminescent materials have been utilized widely in applications, such as cathode ray tubes, fluorescence lamps, vacuum fluorescent display devices, color plasma display panels, and electroluminescent flat-panel displays [10]. There is also a strong commercial desire to produce efficient and lasing blue-light-emitting diodes and short-wave-length laser diodes by exploiting this type of nanomaterial [11].

The luminescent properties of ZrO_2 seem to depend strongly on the preparation methods. Among these stand out the sol-gel process, microwave irradiation and hydrothermal method [12]. In particular hydrothermal process is a promising method for preparation of fine ceramic powder. The powders synthesized by this method have several advantages, for example, the product is homogeneous and highly crystalline and can be obtained directly from a reaction to a relatively low

temperature (< 150 °C), which favors the binding between particles, distribution of particle size, homogeneity of phases, uniform composition, products with high purity and controlled particle morphology, solvent environmentally friendly, low energy cost and lower reaction time [12].

In this study we present the synthesis of pure m-ZrO_2 nanostructures with controlled morphology and high crystallinity structural analysis and optical studies of the nanostructures are performed by various characterization techniques. All the chemicals employed were of analytical grade and used without further purification.

Materials and Methods

ZrO_2 nanostructures were synthesized by a simple hydrothermal route. Initially 4 mL of H_2O_2 was slowly dripped in 1.87 g (0.008 mol) of $ZrO(NO_3)_2.xH_2O$, occur until the complete chemical reaction of hydrolysis. Then was added 100 mL of DI water and the system was homogenized by a magnetic stirrer. After this system was well sealed and transferred to a stove with controlled temperature at 120 ºC for 24h. Finally, the suspension was removed to a petri dish and dried at 60 ºC for 4h.

After the HT processing at 120 ºC for different times, these nanocrystals were structurally characterized by XRD using a Rigaku-DMax/2500PC (Japan) with Cu-Ka radiation (λ = 1.5406 Å) in the 2q range from 10^o to 75^o with scanning rate of 0.02^o s^{-1} exposure total time of 15min and also Rietveld routine was performed in the 2q range from 10^o to 110^o, using an angular step of 0.02^o/s and exposure total time of 90min. The Micro-Raman measurements were recorded using a T-64000 spectrometer (Jobin-Yvon, France) triple monochromator coupled to a CCD detector. The spectra were performed using a 488 nm wavelength of an argon ion laser, keeping its maximum output power at 10 mW. The morphologies were investigated through a FEG-SEM of Carl Zeiss, model supra 35-VP (Germany) operated at 6 kV and with a transmission electron microscopy (TEM), model TECNAI G2 TEM (FEI Corporation, Holland) operated at 200 keV. Photoluminescence measurements were performed through a Monospec 276 monochromator of Thermal Jarrel Ash (USA) coupled to a R446 photomultiplier of Hamamatsu Photonics (Japan). A krypton ion laser of Coherent Innova 90K (USA) (λ = 350 nm) was used as an excitation source, keeping its maximum output power at 500 mW and maximum power on the sample after passing through from optical chopper of 40 mW.

Results and Discussion

Fig.1 shows the XRD profiles of ZrO_2 nanocrystal. All diffraction peaks were indexed to the monoclinic structure with space group P21/c in agreement with the respective Inorganic Crystal Structure Database (ICSD) N*o*. 18190 [13].

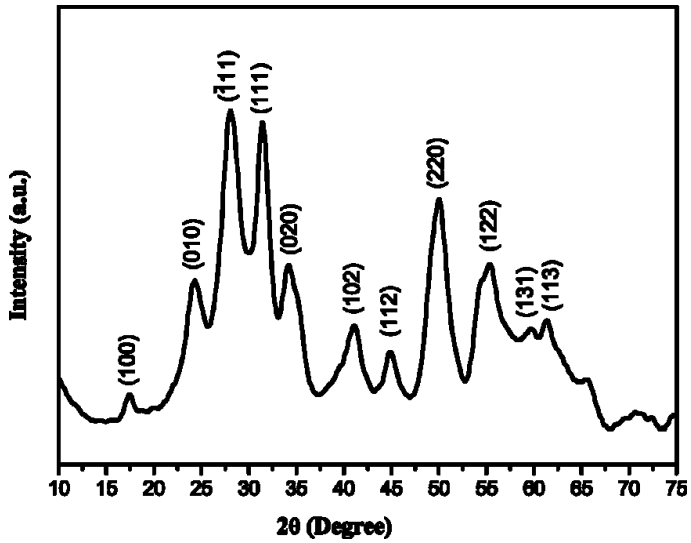

Fig. 1. XRD profiles of ZrO_2 nanocrystal.

The broadening of these peaks implies that the obtained samples are composed by nanoscale structures. No secondary peaks were observed, indicating the obtention of a monophasic system. Also, it is possible to note that these peaks are fairly broad suggesting a presence of nanocrystalline systems and structural ordering at long range, in agreement with other papers reported in the literature for monoclinic ZrO_2 nanoparticles [14, 15].

Fig. 2 shows the Raman spectra of ZrO_2 nanocrystals. The Raman-active phonon modes can be used to estimate the structural order at short range in the materials. According to group theory calculations the ZrO_2 with baddeleyite-type monoclinic structure exhibit 36 different (Raman and infrared) vibrational modes, which are represented by equation (1) below: [16]

$$\Gamma = 9Ag+9Bg+9Au+9Bu \quad (1)$$

where the *Ag* and *Bg* are Raman-active vibration modes, the *A* and *B* modes are nondegenerate, while the *Au* and *Bu* are infrared-active vibration modes. The subscripts "*g*" and "*u*" indicate the parity under inversion in centro symmetric crystals at the center of the Brillouin zone. Therefore, it is expected 18 zone-center Raman-active vibrational modes for the ZrO_2 crystals, as presented in equation (2): [16]

$$\Gamma(Raman) = 9Ag+9Bg \quad (2)$$

As it can be noted in Figure 2, only 10 of the 18 Raman active modes can be detected, the others (1*Ag* and 5*Bg*) Raman vibrational modes were not detectable, probably, due to its low intensities. According to the literature, in Raman spectra of monoclinic ZrO_2 nanocrystalline, the frequencies too high to be related to the first-order silent modes and they are likely the second-order active Raman modes [17]. The active Raman modes at 182, 330, 380, 478, 548 and 611 cm^{-1}, these bands are related to monoclinic structure. These results are agreement with the DRX results.

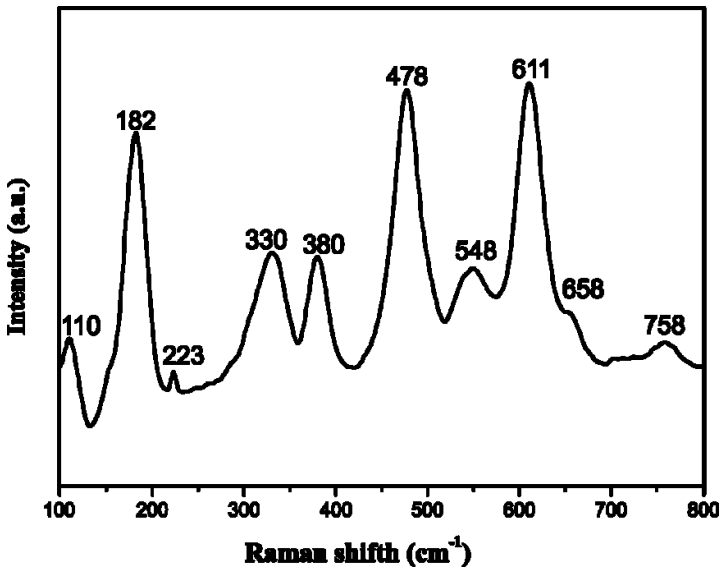

Fig. 2. Raman spectra of ZrO_2 nanocrystal.

Figure 3 show the morphology of the as-prepared ZrO_2 powders observed by transmission electron microscopy (TEM) for ZrO_2 nanocrystals. To check directly the morphology of the nanoparticles, TEM images were collected and showed that this route of synthesis provides well-dispersed nanocrystalline ZrO_2 in nanorods like with oriented attachment as main growth mechanism [18]. It is possible to observe that these nanoparticles are aggregates of small crystallites (< 9 nm). Hu et al. suggested a mechanism to obtain monoclinic zirconia from such small particles, obtaining cube-shaped aggregates of monoclinic zirconium oxide of small crystallites that are formed only after an induction period of approximately 20h [19]. Yashima also suggested that the differences in oxygen deficiency between tetragonal and monoclinic phases are critical to stabilize each structure. As the

oxygen deficiency is modified as the crystallite size changes, it is expected that the stability of the oxide phase should be affected by the particle size also because the oxygen deficiency [20]. However, differently to others routes, the presence of hydrogen peroxide in our synthesis can lead the particles to be richer in oxygen, reducing the oxygen vacancy, and for this reason, inducing the formation of the monoclinic phase preferentially [20].

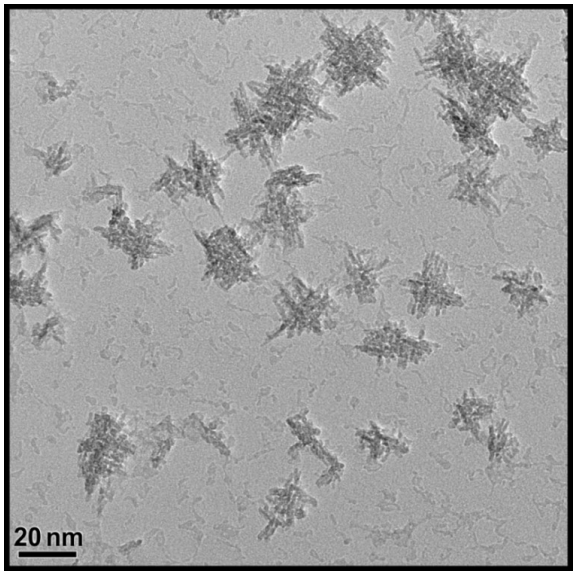

Fig. 3. TEM image of the as-prepared ZrO_2.

Fig. 4 shows the photoluminescence spectra of ZrO_2 nanocrystals. Photoluminescence (PL) technique is suitable to determine the crystalline quality and presence of impurities in the materials, as well as exciton ine structure. The PL spectra are a broadband covering a large part of the visible electromagnetic spectrum, with a maximum emission situated at around 530 nm (green emission). This emission around 530, it should be due to the involvement of mid-gap trap states, such as surface defects and oxygen vacancies. The weak green emission also implies that there are surface defects in ZrO_2. Large amounts of surface defects exist on the as-synthesized nano-ZrO_2 particles because of their high surface area [21].

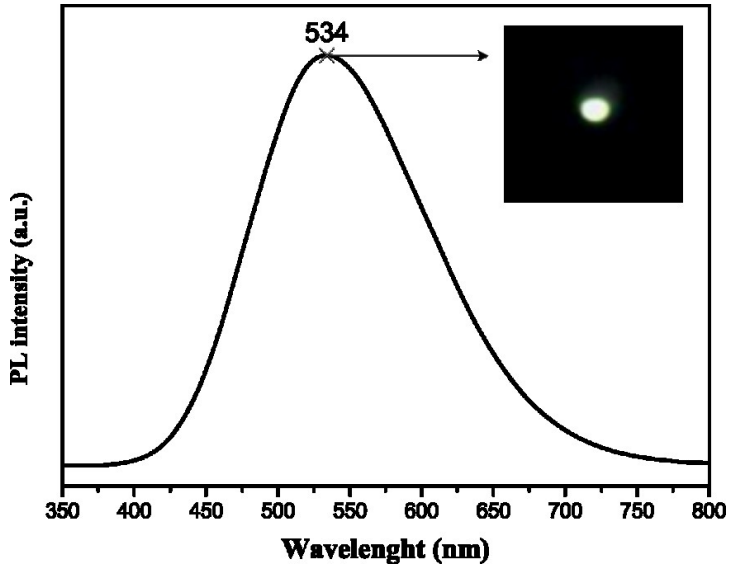

Fig. 4. PL of the as-prepared ZrO_2.

Conclusion

In this work, nanocrystalline zirconia with homogeneous morphology and with small nanocrystallite size was successfully synthesized by a hydrothermal method from zirconyl nitrate. The micrograph shows well-dispersed nanocrystals ZrO_2-shaped nanorods. The average size of ZrO_2 by TEM was measures to be ~8 nm. The PL spectrum of nanarods like ZrO_2 nanostructures shows a broad band covering a large part of the visible spectrum with a maximum situated at 534 nm (green emission). This PL profile suggests an emission mechanism characterized by the participation of several energy levels or light emission centers able to trap electrons within the band gap.

References

[1] Y.J. Liu, R.O.J. Claus:J. Am. Chem. Soc. Vol. 119 (1997), p. 5273.
[2] K.Vanheusden, W.L Warren, C.H Seaeger, D.R Jallant, J.A.Voigt, B.E. Gnade: J. Appl. Phys. Vol. 79 (1996), p. 7983.
[3] J. Liang, Z. Deng, X. Jiang, F. Li, Y. Li: Inorganic Chem. Commu. Vol. 41 (2002), p. 3602.
[4] A.V. Emeline and N. Serpone: Chem. Phys. Lett. Vol. 345 (2001), p. 105.
[5] C. Lin, C. Zhang, d J. Lin: J. Phys. Chem. C Vol. 111 (2007), p. 3300.
[6] S. Shukla, S. Seal, R. Vij, S. Bandyopadhyay: Nano. Lett. Vol. 3 (2003), p. 397.
[7] R.H. French, S.J.Glass, F.S. Ohuchi, Y.-N. Xu, W.Y. Ching: Phys. Rev. B Vol. 49 (1994), p. 5133.
[8] A. Emeline, G.V. Kataeva, A.S. Litke, A.V. Rudakova, V.K. Ryabchuk, N. Serpone: Langmuir Vol. 14 (1998), p. 5011.
[9] C.H. Lu, H.C. Hong, R.J. Jagannathan: J. Mater.Chem. Vol. 12 (2002), p. 2525.
[10] G. Blasse, B.C. Grabmaier: ***Luminescent Materials***. (Springer, Heidelberg 1994).
[11] K. Latha, W. Z. Li: Cryst. Growth Vol. 9 (2009), p. 3874.
[12] M.Z.C. Hu, M.T. Harris, C.H. Byers: J. Colloid and Interf. Sci. Vol. 198 (1998), p. 87.
[13] D.K. Smith, W. Newkirk: Acta. Cryst. Vol. 18 (1965), p. 983.
[14] M. Bhagwat, V. Ramaswamy: Mater. Res. Bull. Vol. 39 (2004), p. 1627.
[15] V. Petkov: Mater.Today Vol. 11 (2008), p. 28.
[16] J. Li, L. Hui, Y. Jian, S. Wenfeng: Univ. Technol. Mater. Sci. Vol. 25 (2010), p. 919.
[17] X. Zhao, D. Vanderbilt: Phys. Rev. B Vol. 65 (2002), p. 075105.
[18] R.D. Purohit, S.A Saha, K. Tyagi: Mater. Sci. Eng B. Vol. 130 (2006), p. 57.
[19] M.Z.C. Hu, M.T. Harris, C.H. Byers: J. Colloid. Interface Sci. Vol. 198 (1998), p. 87.
[20] M. Yashima, S. Tsunekawa: Acta Cryst. B. Vol. 62 (2006), p. 161.
[21] A.K. Singh1 and U.T. Nakate: The Scientific World Journal ID 349457 (2014), p. 1.